

Tumorigenesis and Neoplastic Progression

Leukemic Blasts with the Paroxysmal Nocturnal Hemoglobinuria Phenotype in Children with Acute Lymphoblastic Leukemia

David J. Araten,* Katie J. Sanders,*
Dan Anscher,* Leah Zamechek,*
Stephen P. Hunger,[†] and Sherif Ibrahim[‡]

From the Division of Hematology,* New York University School of Medicine, New York University Langone Clinical Cancer Center and New York VA Medical Center, New York, New York; Children's Hospital Colorado and the Department of Pediatrics,[†] University of Colorado School of Medicine, Aurora, Colorado; and the Department of Pathology,[‡] New York University School of Medicine, New York, New York

It has been proposed that genomic instability is essential to account for the multiplicity of mutations often seen in malignancies. Using the X-linked *PIG-A* gene as a sentinel gene for spontaneous inactivating somatic mutations, we previously showed that healthy individuals harbor granulocytes with the *PIG-A* mutant (paroxysmal nocturnal hemoglobinuria) phenotype at a median frequency (f) of $\sim 12 \times 10^{-6}$. Herein, we used a similar approach to determine f in blast cells derived from 19 individuals with acute lymphoblastic leukemia (ALL) and in immortalized Epstein-Barr virus-transformed B-cell cultures (human B-lymphoblastoid cell lines) from 19 healthy donors. The B-lymphoblastoid cell lines exhibited a unimodal distribution, with a median f value of 11×10^{-6} . In contrast, analysis of the f values for the ALL samples revealed at least two distinct populations: one population, representing approximately half of the samples ($n = 10$), had a median f value of 13×10^{-6} , and the remaining samples ($n = 9$) had a median f value of 566×10^{-6} . We conclude that in ALL, there are two distinct phenotypes with respect to hypermutability, which we hypothesize will correlate with the number of pathogenic mutations required to produce the leukemia. (*Am J Pathol* 2012, 181:1862–1869; <http://dx.doi.org/10.1016/j.ajpath.2012.07.025>)

For a few sentinel genes, such as *HPRT*,^{1,2} *GPA*^{3–5} *XK*,⁶ *HLA*,⁷ and *PIG-A*,⁸ it is possible to use a phenotypic

screen to quantitate the frequency (f) of spontaneously arising mutants in blood cells from healthy individuals. In these models, f values generally range from 1×10^{-6} to $>60 \times 10^{-6}$, depending on the sentinel gene and the age of the individual. Such estimates are critical for quantitative models of carcinogenesis. For example, considering that mutations in n different oncogenes or tumor suppressor genes are required for the development of malignancy, if each one were to occur independently, then the probability of n mutations coinciding in the same cell should approximate \bar{f}^n , where \bar{f} represents the geometric mean of the frequencies for the different oncogenic mutations. Since the adult body has $<10^{14}$ cells, it has been argued that given these measured values for \bar{f} , it would be impossible for malignancy ever to occur if $n > 2$ unless spontaneous mutation rates were to somehow increase during the process of malignant transformation.^{9,10}

Hypermutability could result from environmental mutagenesis or from genetic or epigenetic inactivation of repair genes. Abnormalities in the expression or fidelity of DNA polymerases and/or DNA repair genes^{10,11} could also result in hypermutability. In support of this model, results from cancer genome sequencing projects have generally demonstrated a surprisingly high number of mutations.^{12–14} However, mutations in repair genes or polymerases have not been commonly found. An alternative model to account for the multiplicity of mutations in cancer in the absence of hypermutability would involve successive rounds of clonal selection. Here, each oncogenic mutation would result in a partial growth advantage in a dividing premalignant cell pop-

Supported by NIH grant RO1-CA109258 (D.J.A.), Veterans Affairs Merit Review 11O1BX-000670-01 (D.J.A.), the Michael Saperstein Medical Scholars Award (D.J.A.), and grants to the Children's Oncology Group including the COG Chair's grant (CA98543 to S.P.H.), U10 CA98413 (COG Statistical Center to S.P.H.), and U24 CA114766 (COG Specimen Banking to S.P.H.).

Accepted for publication July 5, 2012.

Address reprint requests to David J. Araten, M.D., Division of Hematology, NYU Langone Clinical Cancer Center, 160 E 34th St, 7th Floor, New York, NY 10016. E-mail: david.araten@nyumc.org.

ulation. According to this model, we might not expect to see a high frequency of phenotypic variants using a sentinel gene that is not itself an oncogene or a tumor suppressor gene.

To evaluate these models, we considered it important to investigate whether there is evidence of hypermutability in *ex vivo* leukemic blasts. However, in applying a phenotypic screen for rare mutants in a leukemic blast population, we are limited by three considerations: i) for some of the sentinel genes mentioned previously herein (eg, *XK* and *GPA*), mutants can be detected only in red blood cells; ii) for *HPRT*, the cells must grow well *in vitro*, which *ex vivo* blast cells do not readily do; and iii) for autosomal genes, the effect of a loss of function mutation on one chromosome may be complemented by the unmutated allele on the homologous chromosome. For a few autosomal genes that have well-characterized polymorphic alleles (eg, *HLA* and *GPA*), it is possible to identify spontaneous loss of one allele—but only in cells from certain individuals who have a specific compound heterozygote genotype.

*PIG-A*¹⁵ does not have these limitations and has several advantages as a sentinel gene for spontaneous somatic mutations. Because *PIG-A* is X-linked (as are *HPRT* and *XK*), a single inactivating mutation can produce the mutant phenotype owing to lyonization in females and hemizyosity in males. *PIG-A* has been well characterized owing to its association with paroxysmal nocturnal hemoglobinuria (PNH), and it is known that a broad spectrum of mutations can inactivate the gene,^{16,17} providing a model for the inactivation of tumor suppressor genes and many of the point mutations that would activate oncogenes. We and others have demonstrated occult populations of cells with the *PIG-A* mutant (PNH) phenotype and genotype in diverse cell types, including granulocytes,⁸ lymphocytes,^{18,19} human B-lymphoblastoid cell lines (BLCLs),^{20,21} and marrow progenitors from normal donors,²² as well as cell lines derived from neoplasms.²³ Animals also harbor rare populations of spontaneously arising blood cells with the *PIG-A* mutant phenotype, and the frequency can be shown to increase as a result of mutagen exposure, as recently reviewed.²⁴

A further advantage of using *PIG-A* as a sentinel gene is that its inactivation confers loss from the cell surface of all proteins that require glycosylphosphatidylinositol (GPI), resulting in a phenotype that can be detected by flow cytometry without a requirement for *in vitro* cell growth. *PIG-A* is widely expressed, and GPI is present in diverse cell types, including primitive hematopoietic cells such as leukemic blasts. In addition, antibodies specific for more than one GPI-linked protein can be used simultaneously, along with the fluorescent aerolysin (FLAER) reagent,²⁵ which binds to the GPI structure directly, to maximize the specificity of any assay. In a previous study using *PIG-A*, we demonstrated hypermutability in many but not all cell lines derived from hematologic malignancies.²⁶ Herein, we applied this approach to determine whether hypermutability can be demonstrated in populations of blasts from patients with ALL.

Materials and Methods

Frozen aliquots of de-identified ficol-sedimented marrow samples were obtained from the Children's Oncology Group repository and from the NYU Department of Pathology in accordance with institutional protocols. All the samples analyzed were known to have been derived from the initial diagnosis of leukemia, before the administration of chemotherapy, except for the sample from patient 2, which was de-identified in a way such that this information was not available. As a control, samples of whole blood were donated by patients with PNH, who provided signed informed consent. Epstein-Barr virus-transformed B-cell lines (BLCLs) were generated using Epstein-Barr virus stock obtained from ATCC to infect lymphocytes obtained from cord blood samples from discarded placentas as well as whole blood from healthy adult donors providing consent as per the Veterans Affairs Medical Center and New York University Institutional Review Board protocol. Six established BLCLs were obtained directly from the Coriell Cell Repositories (Camden, NJ).

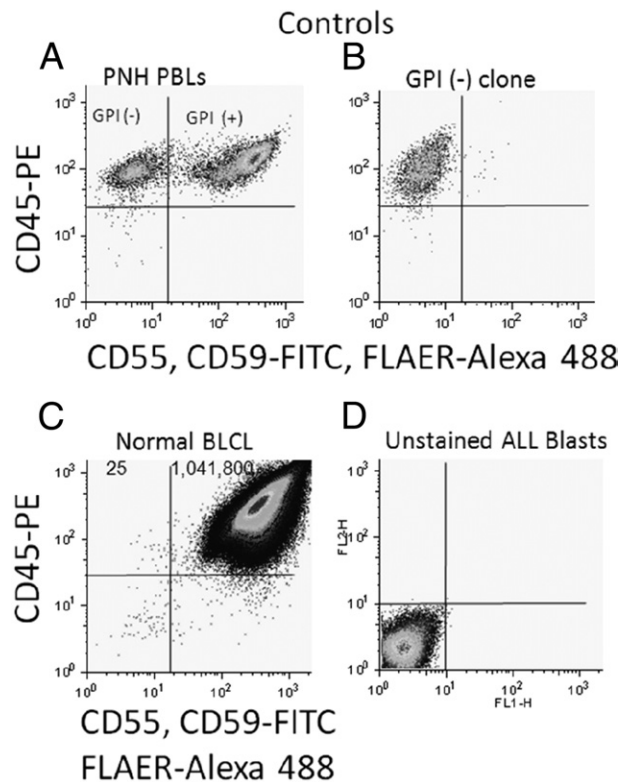


Figure 1. Flow cytometry pseudocolor dot plot analyses of controls. Fluorescein isothiocyanate (FITC) and Alexa 488 register on FL1 (horizontal axis) and reflect the density of the GPI-linked proteins (CD55 and CD59) and the GPI anchor itself, respectively, on the surface of the cell. Phycoerythrin (PE) registers on FL2 (vertical axis), reflecting the density of CD45, a non-GPI-linked membrane protein. GPI⁻ cells register in the top left quadrant, and GPI⁺ cells register in the top right quadrant. **A:** Peripheral blood lymphocytes (PBLs) isolated from a patient with PNH. There are two distinct populations representing GPI⁺ and GPI⁻ cells. **B:** A spontaneously arising GPI⁻ clone of the Jurkat cell line registering in the top left quadrant. **C:** A representative BLCL derived from a healthy donor (BLCL 12): most of the cells are GPI⁺, with a small but distinct subpopulation of GPI⁻ cells registering in the top left quadrant. The frequency of these spontaneously arising phenotypic variants is 24×10^{-6} in this example. **D:** Unstained thawed blasts from a patient with ALL.

Table 1. BLCL Controls from Healthy Donors

Cell line	Sex	Age of donor (years)	No. of gated GPI ⁻ cells	Total No. of gated cells	Frequency of GPI ⁻ cells per million ($f \times 10^6$)
BLCL 1	F	77	36	1,329,700	27
BLCL 2	M	73	11	1,319,757	8.3
BLCL 3	M	29	13	1,240,805	11
BLCL 4	M	71	174	1,165,695	149
BLCL 5	NA	NA	1	1,091,817	0.9
BLCL 6	NA	Cord blood	3	750,602	4.0
BLCL 7	NA	Cord blood	0	396,746	0.0
BLCL 8	NA	Cord blood	5	663,771	7.5
BLCL 9	NA	Cord blood	55	884,288	62
BLCL 10	M	NA	8	504,941	16
BLCL 11	F	83	24	789,240	30
BLCL 12	F	60	25	1,041,825	24
BLCL 13	M	31	8	738,969	11
BLCL 14 (GM03299)	F	8	6	1,882,614	3.2
BLCL 15 (GM03715)	F	12	17	1,411,330	12
BLCL 16 (GM00130)	M	25	176	1,671,951	105
BLCL 17 (GM14583)	M	31	3	1,342,490	2.2
BLCL 18 (GM00131)	F	23	11	1,642,549	6.7
BLCL 19 (GM14537)	M	20	22	1,450,815	15

F, female; M, male; NA, not available.

To generate BLCLs, for the first several weeks, until the BLCLs started to grow and exhaust the media, cyclosporine was added at a concentration of 2 $\mu\text{g}/\text{mL}$ to prevent T-cell activation. The cells were then grown in RPMI 1640 medium with 15% fetal bovine serum, L-glutamine, penicillin-streptomycin, and nonessential amino acids.

Samples from patients with ALL were first thawed and diluted into Dulbecco's modified Eagle's medium media with at least 20% fetal bovine serum and then were incubated with the Alexa 488-conjugated FLAER reagent (Pinewood Scientific Services Inc, Victoria, BC, Canada) for 30 minutes at 37°C at a concentration of 5×10^{-7} mol/L. The cells were then placed on ice for the remainder of the experiment and then were incubated with

mouse anti-CD55 and anti-CD59 antibodies (1:20 dilution; AbD Serotec, Raleigh, NC). The cells were then washed twice and incubated with fluorescein isothiocyanate-conjugated rabbit-anti-mouse immunoglobulin (1:5 dilution; Dako, Carpinteria, CA). The cells were washed twice again, were incubated with phycoerythrin-conju-

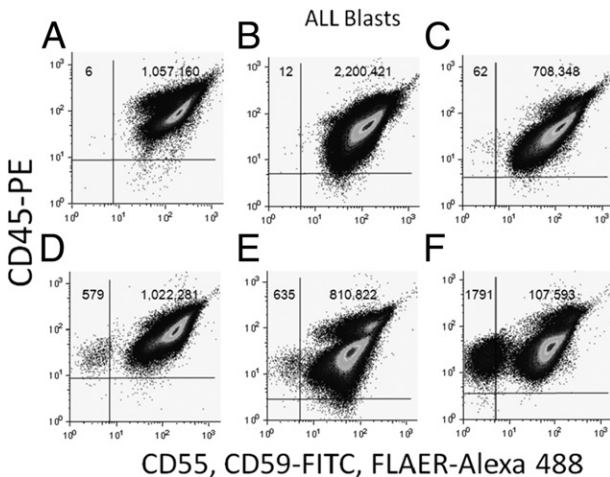


Figure 2. Flow cytometry pseudocolor dot plot analyses of samples derived from ALL blast populations. **A** and **B**: Representative examples of samples with a low frequency of spontaneously arising GPI⁻ phenotypic variants (patients 7 and 17, respectively). **C**: An example of a sample with an intermediate-sized population of GPI⁻ phenotypic variants (patient 11). **D-F**: Representative examples of samples exhibiting a very high frequency of GPI⁻ phenotypic variants (patients 5, 14, and 19, respectively). FITC, fluorescein isothiocyanate; PE, phycoerythrin.

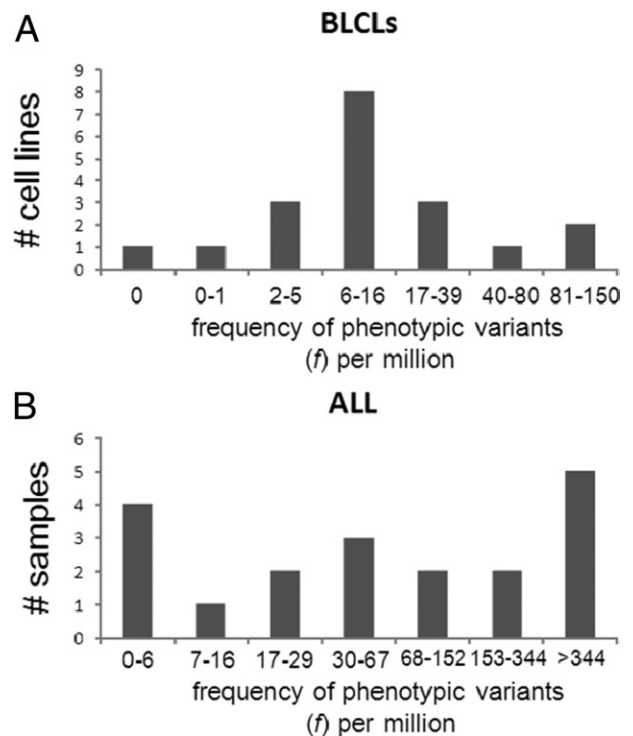


Figure 3. Histogram of f values for BLCL and ALL samples. **A**: Using a λ value of 0.25 in a Box-Cox transformation, f values for the BLCLs are unimodal and nearly symmetrical, and they fall on a nearly straight line in a q-q plot, suggesting that these values are near normally distributed. **B**: There is no transformation that could produce a unimodal symmetrical distribution for the f values measured in ALL samples. Using a log transformation of the f values, it is seen that the distribution is bimodal or trimodal.

gated murine anti-CD45 (1:5 dilution; AbD Serotec), and were washed again. To ensure that the entire sample population came in contact with the reagents, antibodies were added to pelleted cells, which were resuspended, briefly centrifuged, and then resuspended again at the start of each incubation. Propidium iodide was added at a concentration of 0.1 $\mu\text{g}/\text{mL}$ before analysis using a FACScan flow cytometer (BD Biosciences, San Jose, CA). As a control, using this protocol, we stained lymphocytes from a patient with PNH, BLCLs from healthy donors, the T-cell leukemia line Jurkat, and a GPI⁻ subclone of Jurkat that had been selected with proaerolysin. By this approach, GPI⁻ cells appear in the top left quadrant and GPI⁺ cells appear in the top right quadrant. Of note, the emission spectrums of Alexa 488 and fluorescein isothiocyanate are extremely close, allowing for detection of both fluorochromes together in a single channel (FL1). When analyzing ALL blasts and control BLCLs from healthy donors, we gated on cells based on forward and side scatter, and we excluded dead cells, which take up propidium iodide, which registers in FL3.

Voltage settings were applied to the photomultiplier tubes such that unstained blast cells would exhibit mean FL1 and FL2 values of ~ 2.5 so that $>80\%$ of the unstained cells would exhibit FL1 values <5 (Figure 1D). In studies of spontaneously arising GPI⁻ cell populations in other cell types, we have found that after appropriate fluorochrome compensation, GPI⁻ cells can be reproducibly identified as having $<4\%$ of the fluorescence of the wild-type population. We, therefore, defined GPI⁻ cells as having $<4\%$ of the FL1 fluorescence of the wild-type population; in cases where this value would be <5 , we used a value of 5 fluorescence units to define the GPI⁻ cells based on the characteristics of unstained blast cells. To exclude cells with a global defect in membrane proteins, we gated on CD45⁺ events, excluding any cells with an FL2 fluorescence $<10\%$ of the mean of the overall population, which allowed inclusion of $\geq 99.7\%$ of the analyzed cells. To maximize the chances of identifying rare events, we aimed to include at least 1 million gated events in each analysis. The frequency of phenotypic variants was calculated as the number of live CD45⁺ GPI⁻ events divided by the total number of live CD45⁺ cells analyzed.

Results

As expected, analysis of peripheral blood lymphocytes from a patient with PNH who was known to have a substantial PNH clone in the lymphocyte, granulocyte, and red blood cell lineages revealed two distinct populations with respect to expression of the GPI-linked proteins CD55 and CD59 and uptake of the FLAER reagent (Figure 1A). Similarly, a GPI⁻ subclone of Jurkat registered in the top left quadrant (Figure 1B), whereas the parental Jurkat culture registered in the top right quadrant (data not shown).

We then analyzed Epstein-Barr virus-immortalized BLCLs from healthy donors. A representative example is shown in Figure 1C, where most of the cells are seen to

express GPI-linked proteins, take up the FLAER reagent, and express the transmembrane protein CD45. Almost the entire population, therefore, registers in the top right quadrant. However, there are rare events in the upper left quadrant that appear phenotypically identical to the control GPI⁻ cells in Figure 1, A and B. Twenty-five such events were counted in 1,041,825 cells analyzed, and the \bar{f} value of these spontaneously arising GPI⁻ phenotypic variants in this example is, therefore, 24×10^{-6} .

In a panel of 19 BLCLs from healthy donors, a median of 1.2 million gated events were analyzed (range, 0.4 million to 1.9 million). In all but one BLCL cell line, at least one spontaneously appearing GPI⁻ event was identified that registered in the top left quadrant. The mean frequency of these phenotypic variants was 26×10^{-6} , with a median value of 11×10^{-6} and a range of 0 to 149×10^{-6} (Table 1). Using a λ value of 0.25 in a Box-Cox transformation, this distribution of values was unimodal and symmetrical, possibly with one high outlier, and the transformed data plotted on a q-q plot demonstrated a nearly straight line, suggesting a near normal distribution.

We also applied this analysis to ALL blasts (Figure 2). Of the 25 available frozen samples, 6 had a lack of viability, extensive cell clumping after thawing, insufficient cells for analysis, or a tail of the distribution curve with respect to FL1 fluorescence that precluded discrimination of GPI⁺ from GPI⁻ cells. In the remaining 19 cases (4 cases of T-cell ALL and 15 cases of B-lineage ALL), it was possible to identify spontaneously arising phenotypic variants. Looking at the \bar{f} values, the distribution clearly differed from that of the values derived from the analysis of BLCLs from healthy donors. Herein, the \bar{f} values spanned four orders of magnitude, ranging from 2.5×10^{-6} to $16,374 \times 10^{-6}$. The mean value was 1046×10^{-6} , and the median value was 65×10^{-6} . The \bar{f} values for the ALL samples, overall, were significantly higher than those for the BLCLs ($P = 0.03$, 1-sided Mann-Whitney U -test). In contrast to the distribution obtained for the BLCLs (Figure 3A), using different possible λ values ranging from -1 to 1 in the Box-Cox formula, there was no transformation that could produce a straight line on the q-q plot or a histogram with a unimodal distribution for the ALL samples (Figure 3B). The 10 ALL samples with the lowest \bar{f} values had a median \bar{f} value of 13×10^{-6} . Representative samples with a low frequency of GPI⁻ variants are shown in Figure 2, A and B. The remaining nine samples had a median \bar{f} value of 566×10^{-6} . Representative samples with a high frequency of phenotypic variants are shown in Figure 2, D-F. Using a log transformation of the \bar{f} values, it is seen that there are at least two distinct populations (Figure 3B). In fact, the distribution may be trimodal, and Figure 2C shows a representative sample with an intermediate frequency of phenotypic variants, in this case 88×10^{-6} .

Discussion

We have taken advantage of the unique properties of the *PIG-A* gene to develop a novel sensitive assay for the presence of phenotypic variants among leukemic blasts from

Table 2. Samples from Patients with Leukemia

Patient no./sex/ age (years)	WBCs ($\times 10^3$ per μL)	Lineage	Metaphase cytogenetics	<i>BCR-ABL</i> (FISH)
1/M/41	NA	B	NA	Positive
2/F/13	NA	T	NA	NA
3/M/18	NA	T	t(13q;18q)	Negative
4/M/4	NA	B	NA	NA
5/M/15	4.5	B	NA	Negative
6/F/4.5	8.6	B	NA	Negative
7/F/7	2.8	B	NA	Negative
8/M/3.5	38	B	47,XY,+5[16]/46,XY[4]	Negative
9/F/6	588	T	46, XX [40]	Negative
10/M/3	18	B	52,XX,+X,+4,+14,+17,+21,+21[8]/46,XY[4]	Negative
11/M/9	1.9	B	NA	Negative
12/F/4	5.8	B	46, XX[20]	Negative
13/M/11	4.8	T	85~87,XXYY,-4,-11,-15,-21[CP18]/46,XY[2]	Negative
14/F/2	63	B	NA	Negative
15/F/5	23	B	46, XX[14]	Negative
16/M/4	13	B	NA	Negative
17/M/3	53	B	52,XY,+X,DUP(1)(q21q42),+10,+14,+17,+21,+21[4]/53,IDEM,+3[4]	Negative
18/F/19	9.3	B	58,XX,+X,+4,+6,+8,+9,+10,+11,+14,+14,DER(16) t(11;16)(q21;q22),ADD(17)(p12),+18,+21,+21[17]/46,XX[2]	Negative
19/M/17	3.9	B	46,XY,t(4;11)(q27;q24),DEL(6)(q21),t(13;14)(q32;q13),ADD(15)(q26)[4]/46,XY[6]	Negative

(table continues)

F, female; M, male; FISH, fluorescence *in situ* hybridization; NA, not available; WBC, white blood cell.

patients with ALL. Because *PIG-A* mutations disrupt the synthesis of the GPI structure and the expression of GPI-linked membrane proteins, the *PIG-A* mutant phenotype can be detected by flow cytometry using monoclonal antibodies against GPI-linked proteins together with FLAER, a fluorescent reagent that binds to GPI directly. This approach allows for screening of a large number of cells to identify rare, spontaneously arising phenotypic variants, which is otherwise not possible to do. Herein we found two distinct patterns. Approximately half of the samples we analyzed exhibited a frequency of phenotypic variants similar to results obtained from nonmalignant blood cells from healthy donors. The other half of the samples we analyzed demonstrated a high frequency of spontaneously arising GPI⁻ cells, which is highly suggestive of genomic instability.

The simplest interpretation of these data is that there are two different pathways to developing leukemia. In the first case, a small number of mutations—perhaps only one mutation in addition to a translocation¹³—are sufficient to initiate the process of leukemogenesis. In this case, hypermutability might not be necessary, and nononcogenic mutations in genes such as *PIG-A* will be rare, with a frequency comparable with that of nonmalignant cells. In the second pathway, a large number of oncogenic mutations are required, which could most easily occur as a result of genomic instability, which will be reflected by an increased number of mutations in oncogenes and an increase in nononcogenic mutations.²⁷ In this pathway, we would, therefore, expect an increased frequency of GPI⁻ phenotypic variants. Individuals with germline variations in repair genes resulting in constitutional hypermutability²⁰ and those with acquired repair defects occurring specifically in the cells of origin of the

malignancy could achieve the requisite number of oncogenic mutations through this second pathway.

It is possible that an initial oncogenic translocation will determine whether the leukemia demonstrates a high or a low mutator phenotype: for example, leukemias harboring the t(12;21) translocation resulting in the *ETV6/RUNX1* (*TEL-AML1*) fusion have been shown to have a higher number of deletion mutations than those with an *MLL* translocation.¹³ Indeed, herein we found that four of five of the samples harboring the *ETV6/RUNX1* translocation (patients 4, 6, 14, 15, and 19 in Table 2) demonstrated a markedly elevated \bar{f} value, as was the case for the sample from patient 1, which harbored a *BCR-ABL* translocation. The *BCR-ABL* translocation has recently been associated with intratumoral genetic diversity,²⁸ and a mechanism has been proposed whereby the BCR-ABL fusion protein directly results in oxidative stress and secondary mutations.²⁹ Two of the samples we analyzed were considered to be hyperdiploid based on trisomies of chromosomes 4 and 10 (patients 13 and 18), and both of these had a low \bar{f} value. We believe that with a large number of samples, each harboring the same cytogenetic abnormality, we may be able to investigate the biological factors associated with hypermutability using this method.

We believe that an elevation in f , as detected in this assay, is due to an increase in the mutation rate rather than increased cell turnover. In a previous work using cell lines, we were able to control for cell divisions, measure the mutation rate directly, and demonstrate that it is frequently, but not universally, elevated in hematologic malignancies.²⁶ We recently analyzed the mutation rate in a panel of cell lines derived from Burkitt neoplasms and found that the distribution of mutation rates in this type of

Table 2. *Continued*

<i>MLL</i> (FISH)	Trisomy 4 and 10 (FISH)	<i>ETV6/RUNX1</i> (FISH)	Hypodiploid (FISH)	No. of gated GPI ⁻ cells	Total no. of gated cells	Frequency of GPI ⁻ cells per million ($f \times 10^6$)
NA	NA	NA	NA	510	1,844,838	276
NA	NA	NA	NA	16	331,368	48
NA	NA	NA	NA	49	1,618,408	30
NA	NA	Positive	NA	148	244,609	605
Negative	Negative	Negative	No	579	1,022,860	566
Negative	NA	Positive	No	13	749,933	17
Negative	Negative	Negative	No	6	1,057,166	5.7
Negative	Negative	Negative	No	133	2,059,699	65
Negative	Negative	Negative	No	83	983,522	84
Negative	Negative	Negative	No	2	787,833	2.5
Negative	Negative	Negative	No	62	708,410	88
Negative	Negative	Negative	No	200	1,196,416	167
Negative	Positive	Negative	No	24	1,242,719	19
Negative	Negative	Positive	No	635	811,457	783
Negative	Negative	Positive	No	1053	1,438,327	732
Negative	Negative	Negative	No	8	1,917,780	4.2
Negative	Negative	Negative	No	12	2,200,433	5.5
Negative	Positive	Negative	No	2	220,314	9.1
Negative	Negative	Positive	No	1791	109,384	16,374

malignancy is bimodal as well (manuscript in preparation). In studying ALL, we cannot control for cell divisions because *ex vivo* leukemic cells do not often adapt to tissue culture. However, the control cells, the BLCLs, had been growing well in culture for a median of 5 months before they were analyzed. These BLCLs did not demonstrate any increase in \bar{f} compared with \bar{f} values from previous work in granulocytes^B or estimates of \bar{f} using other model systems.^{1-7,20,30,31} Indeed, although they were growing rapidly *in vitro*, their \bar{f} values overall were significantly lower than those of the ALL samples, suggesting that hypermutability in a subgroup of ALL samples is likely to be a feature of the malignant phenotype rather than of proliferation *per se*.

The assay is set up to detect mutations in the *PIG-A* gene, which can be inactivated by a broad spectrum of mutations,^{16,17} including nonsense, missense, and splice site mutations; frameshifts; small in-frame deletions; and very large deletions. Although in PNH the GPI⁻ phenotype, as a rule, results from mutations in *PIG-A*, strictly speaking, the GPI⁻ phenotype could be produced by loss (or epigenetic silencing³²) of any of the ~20 genes involved in GPI anchor synthesis³³⁻³⁵ or the genes necessary for GPI trafficking.³⁶ However, except for *PIG-A*, these genes are autosomal³⁴ and would probably require biallelic inactivation to produce the GPI⁻ phenotype, which would probably occur less frequently than a single *PIG-A* mutation.

We cannot completely rule out the possibility that the GPI⁻ phenotype could be positively or negatively selected at various stages in the development of leukemia, which could increase or decrease, respectively, the \bar{f} values we observe. However, it is widely believed that

PIG-A mutations are growth neutral *in vivo* and *in vitro*^{20,37-39} in situations apart from the special case of aplastic anemia.⁴⁰ Of note, *PIG-A* is not emerging as a driver gene in genome-wide analyses,^{12,41-46} arguing that selection in favor of *PIG-A* mutants is an unlikely explanation for these findings. Although it is highly likely that an increase in the frequency of phenotypic variants as measured herein is due to genomic or epigenetic instability, we cannot say that a low \bar{f} value rules out all forms of hypermutability. Specifically, a propensity toward translocations and gene amplifications would probably escape detection here. In addition, theoretically, it is possible that successive rounds of clonal selection could periodically reduce the observed frequency of phenotypic variants, as has been reported in yeast growing in culture over a prolonged period.⁴⁷

Another caveat is that we cannot be certain that *PIG-A* is reflective of the mutation rate in other genes. This is an issue any time a sentinel gene is chosen, particularly because a phenotypic screen is possible for only a very few genes for comparison. Of note, our studies on the mutation rate in nonmalignant human cells using *PIG-A* have generally corresponded to mathematical models of the mutation rate in *HPRT*.²⁰ Although it is possible to perform deep sequencing for a large number of genes to demonstrate intratumoral diversity, in a recent study using this technology,⁴⁸ this approach had a sensitivity of detecting a heterozygous point mutation of ~1 per 166 cells, below which mutations could not be distinguished from sequencing errors. Random mutation capture is a highly sensitive assay developed by Bielas et al²⁷ to detect rare point mutations at recognition sites for a highly efficient restriction enzyme and, in the future, may

complement the assay described herein. However, random mutation capture is unlikely to be as easily implemented as an assay based on flow cytometry.

Despite these caveats, we believe that we have developed the first clinically applicable test that is reflective of hypermutability and tumoral genetic diversity in leukemic blasts, and we believe that the parameter we measured herein is likely to be clinically relevant. For example, a high \bar{f} value might correlate with the probability of mutations in genes associated with relapse and chemotherapy resistance,^{45,49} and, indeed, mutations in *PIG-A* itself could confer resistance to alemtuzumab, which targets CD52, a GPI-linked protein.¹⁸ In fact, there are recent data from an animal model of human ALL that this may occur.⁵⁰ Conversely, leukemias that demonstrate hypermutability may be more susceptible to the effects of DNA-damaging drugs, such as alkylating agents and anthracyclines, that might increase the mutation rate above the threshold at which viability would be compromised. These findings suggest that it will be possible to apply this analysis at the time of routine phenotyping of leukemia and to investigate these questions further by following patient outcomes prospectively.

Acknowledgments

We thank Drs. Meenakshi Devidas, I-Ming Chen, and Mignon Loh (Children's Oncology Group) for their assistance coordinating the sharing of samples and Bridget Lane for her assistance obtaining blood samples from healthy donors.

References

1. Albertini R, Castle K, Borchering W: T-cell cloning to detect the mutant 6-thioguanine-resistant lymphocytes present in human peripheral blood. *Proc Natl Acad Sci U S A* 1982, 79:6617–6621
2. Morley A, Cox S, Holliday R: Human lymphocytes resistant to 6-thioguanine increase with age. *Mech Ageing Dev* 1982, 19:21–26
3. Langlois R, Bigbee W, Jensen R: Flow cytometric characterization of normal and variant cells with monoclonal antibodies specific for glycophorin A. *J Immunol* 1985, 134:4009–4017
4. Langlois R, Bigbee W, Jensen R: Measurements of the frequency of human erythrocytes with gene expression loss phenotypes at the glycophorin A locus. *Hum Genet* 1986, 74:353–362
5. Vickers MA, Hoy T, Lake H, Kyoizumi S, Boyse J, Hewitt M: Estimation of mutation rate at human glycophorin A locus in hematopoietic stem cell progenitors. *Environ Mol Mutagen* 2002, 39:333–341
6. Araten D, Sanders K, Pu J, Lee S: Spontaneously arising red cells with a McLeod-like phenotype in normal donors. *Mutat Res* 2009, 671:1–5
7. Grist S, McCarron M, Kutlaca A, Turner D, Morley A: In vivo human somatic mutation: frequency and spectrum with age. *Mutat Res* 1992, 266:189–196
8. Araten D, Nafa K, Lake H, Pakdeesuwan K, Luzzatto L: Clonal populations of hematopoietic cells with paroxysmal nocturnal hemoglobinuria genotype and phenotype are present in normal individuals. *Proc Natl Acad Sci U S A* 1999, 96:5209–5214
9. Loeb L, Bielas J, Beckman R, Research C: Cancers exhibit a mutator phenotype: clinical implications. *Cancer Res* 2008, 68:3551–3557
10. Loeb LA: Mutator phenotype may be required for multistage carcinogenesis. *Cancer Res* 1991, 51:3075–3079
11. Bhattacharyya N, Skandalis A, Ganesh A, Groden J, Meuth M: Mutator phenotypes in human colorectal carcinoma cell lines. *Proc Natl Acad Sci U S A* 1994, 91:6319–6323
12. Ley T, Mardis E, Ding L, Fulton B, McLellan M, Chen K, et al: DNA sequencing of a cytogenetically normal acute myeloid leukaemia genome. *Nature* 2008, 456:66–72
13. Mullighan CG, Goorha S, Radtke I, Miller CB, Coustan-Smith E, Dalton JD, Girtman K, Mathew S, Ma J, Pounds SB, Su X, Pui CH, Relling MV, Evans WE, Shurtleff SA, Downing JR: Genome-wide analysis of genetic alterations in acute lymphoblastic leukaemia. *Nature* 2007, 446: 758–764
14. Sjöblom T, Jones S, Wood LD, Parsons DW, Lin J, Barber T, Mandelker D, Leary RJ, Ptak J, Silliman N, Szabo S, Buckhaults P, Farrell C, Meeh P, Markowitz SD, Willis J, Dawson D, Willson JKV, Gazdar AF, Hartigan J, Wu L, Changsheng L, Parmigiani G, Park BH, Bachman KE, Papadopoulos N, Vogelstein B, Kinzler KW, Velculescu VE: The consensus coding sequences of human breast and colorectal cancers. *Science* 2006, 314:268–274
15. Miyata T, Takeda J, Iida Y, Yamada N, Inoue N, Takahashi M, Maeda K, Kitani T, Kinoshita T: The cloning of *PIG-A*, a component in the early step of GPI-anchor biosynthesis. *Science* 1993, 259:1318–1320
16. Luzzatto L, Nafa K: Genetics of PNH, ch 2. Edited by Young, N Moss. J San Diego, Academic Press, 2000, pp 21–47
17. O'Keefe C, Sugimori C, Afable M, Clemente M, Shain K, Araten D, List A, Epling-Burnette P, Maciejewski J: Deletions of Xp22.2 including *PIG-A* locus lead to paroxysmal nocturnal hemoglobinuria. *Leukemia* 2011, 25:379–382
18. Rawstron AC, Rollinson SJ, Richards S, Short MA, English A, Morgan GJ, Hale G, Hillmen P: The PNH phenotype cells that emerge in most patients after CAMPATH-1H therapy are present prior to treatment. *Br J Haematol* 1999, 107:148–153
19. Ware RE, Pickens CV, DeCastro CM, Howard TA: Circulating *PIG-A* mutant T lymphocytes in healthy adults and patients with bone marrow failure syndromes. *Exp Hematol* 2001, 29:1403–1409
20. Araten DJ, Golde DW, Zhang RH, Thaler HT, Gargiulo L, Notaro R, Luzzatto L: A quantitative measurement of the human somatic mutation rate. *Cancer Res* 2005, 65:8111–8117
21. Araten DJ, Luzzatto L: The mutation rate in *PIG-A* is normal in patients with paroxysmal nocturnal hemoglobinuria (PNH). *Blood* 2006, 108: 734–736
22. Hu R, Mukhina GL, Piantadosi S, Barber JP, Jones RJ, Brodsky RA: *PIG-A* mutations in normal hematopoiesis. *Blood* 2005, 105:3848–3854
23. Chen R, Eshleman JR, Brodsky RA, Medof ME: Glycosylphosphatidylinositol-anchored protein deficiency as a marker of mutator phenotype in cancer. *Cancer Res* 2001, 61:654–658
24. Peruzzi B, Araten D, Notaro R, Luzzatto L: The use of *PIG-A* as a sentinel gene for the study of the somatic mutation rate and of mutagenic agents in vivo. *Mutat Res* 2010, 705:3–10
25. Brodsky R, Mukhina G, Li S, Nelson K, Chirrazzi P, Buckley J, Borowitz M: Improved detection and characterization of paroxysmal nocturnal hemoglobinuria using fluorescent aerolysin. *Am J Clin Pathol* 2000, 114:459–466
26. Araten D, Martinez-Climent J, Holm E, DiTata K, Sanders K: A quantitative analysis of genomic instability in lymphoid and plasma cell neoplasms based on the *PIG-A* gene. *Mutat Res* 2010, 686:1–8
27. Bielas JH, Loeb KR, Rubin BP, True LD, Loeb LA: Human cancers express a mutator phenotype. *Proc Natl Acad Sci U S A* 2006, 103:18238–18242
28. Notta F, Mullighan C, Wang J, Poepl A, Doulatov S, Phillips L, Ma J, Minden M, Downing J, Dick JE: Evolution of human BCR-ABL1 lymphoblastic leukaemia-initiating cells. *Nature* 2011, 469:362–367
29. Nowicki M, Falinski R, Koptyra M, Slupianek A, Stoklosa T, Gloc E, Nieborowska-Skorska M, Blasiak J, Skorski T: BCR/ABL oncogenic kinase promotes unfaithful repair of the reactive oxygen species-dependent DNA double-strand breaks. *Blood* 2004, 104:3746–3753
30. Albertini R, Nicklas J, O'Neill J, Robison S: In vivo somatic mutations in humans: measurement and analysis. *Annu Rev Genet* 1990, 24: 305–326
31. Morley A, Trainor K, Seshadri R, Ryall R: Measurement of in vivo mutations in human lymphocytes. *Nature* 1983, 302:155–156
32. Hu R, Mukhina G, Lee S, Jones R, Englund P, Brown P, Sharkis S, Buckley J, Brodsky R: Silencing of genes required for glycosylphosphatidylinositol anchor biosynthesis in Burkitt lymphoma. *Exp Hematol* 2009, 37:423–434
33. Almeida A, Murakami Y, Layton D, Hillmen P, Sellick G, Maeda Y, Richards S, Patterson S, Kotsianidis I, Mollica L, Crawford D, Baker A,

- Ferguson M, Roberts I, Houlston R, Kinoshita T, Karadimitris A: Hypomorphic promoter mutation in PIGM causes inherited glycosylphosphatidylinositol deficiency. *Nat Med* 2006, 12:846–851
34. Kinoshita T: Overview of PNH, Part 1, in paroxysmal nocturnal hemoglobinuria and related disorders: molecular aspects of pathogenesis. Edited by Omine, M Kinoshita, T. Tokyo, Springer-Verlag, 2003, p. 6
35. Kinoshita T, Inoue N: Dissecting and manipulating the pathway for glycosylphosphatidylinositol-anchor biosynthesis. *Curr Opin Chem Biol* 2000, 4:632–638
36. Tashima Y, Taguchi R, Murata C, Ashida H, Kinoshita T, Maeda Y: PGAP2 is essential for correct processing and stable expression of GPI-anchored proteins. *Mol Biol Cell* 2006, 17:1410–1420
37. Araten DJ, Bessler M, McKenzie S, Castro-Malaspina H, Childs BH, Boulad F, Karadimitris A, Notaro R, Luzzatto L: Dynamics of hematopoiesis in paroxysmal nocturnal hemoglobinuria (PNH): no evidence for intrinsic growth advantage of PNH clones. *Leukemia* 2002, 16:2243–2248
38. Keller P, Payne JL, Tremml G, Greer PA, Gaboli M, Pandolfi PP, Bessler M: FES-Cre targets phosphatidylinositol glycan class A (PIGA) inactivation to hematopoietic stem cells in the bone marrow. *J Exp Med* 2001, 194:581–590
39. Rosti V, Tremml G, Soares V, Pandolfi P, Luzzatto L: Murine embryonic stem cells without pig-a gene activity are competent for hematopoiesis with the PNH phenotype but not for clonal expansion. *J Clin Invest* 1997, 100:1028–1036
40. Rotoli B, Luzzatto L: Paroxysmal nocturnal haemoglobinuria. *Baillieres Clin Haematol* 1989, 2:113–138
41. Chapman M, Lawrence M, Keats J, Cibulskis K, Sougnez C, Schinzel A, et al: Initial genome sequencing and analysis of multiple myeloma. *Nature* 2011, 471:467–472
42. Dunwell T, Hesson L, Rauch T, Wang L, Clark R, Dallol A, Gentle D, Catchpole D, Maher E, Pfeifer G, Latif F: A genome-wide screen identifies frequently methylated genes in haematological and epithelial cancers. *Mol Cancer* 2010, 9:44
43. Mardis E, Ding L, Dooling D, Larson D, McLellan M, Chen K, et al: Recurring mutations found by sequencing an acute myeloid leukemia genome. *N Engl J Med* 2009, 361:1058–1066
44. Mullighan C, Miller C, Radtke I, Phillips L, Dalton J, Ma J, White D, Hughes TP, Beau ML, Pui C, Relling MV, Shurtleff S, Downing J: BCR-ABL1 lymphoblastic leukaemia is characterized by the deletion of Ikaros. *Nature* 2008, 453:110–114
45. Mullighan C, Phillips L, Su X, Ma J, Miller C, Shurtleff S, Downing J: Genomic analysis of the clonal origins of relapsed acute lymphoblastic leukemia. *Science* 2008, 322:1377–1380
46. Puente XS, Pinyol M, Quesada V, Conde L, Ordonez GR, Villamor N, et al: Whole-genome sequencing identifies recurrent mutations in chronic lymphocytic leukaemia. *Nature* 2011, 475:101–105
47. Paquin C, Adams J: Frequency of fixation of adaptive mutations is higher in evolving diploid than haploid yeast populations. *Nature* 1983, 302:495–500
48. Walter M, Shen D, Ding L, Shao J, Koboldt D, Chen K, Larson D, McLellan M, Dooling D, Abbott R, Fulton R, Magrini V, Schmidt H, Kalicki-Veizer J, O'Laughlin M, Fan X, Grilot M, Witowski S, Heath S, Frater J, Eades W, Tomasson M, Westervelt P, DiPersio J, Link D, Mardis E, Ley T, Wilson R, Graubert T: Clonal architecture of secondary acute myeloid leukemia. *N Engl J Med* 2012, 366:1090–1098
49. Hogan L, Meyer J, Yang J, Wang J, Wong N, Yang W, Condos G, Hunger S, Raetz E, Saffery R, Relling M, Bhojwani D, Morrison D, Carroll W: Integrated genomic analysis of relapsed childhood acute lymphoblastic leukemia reveals therapeutic strategies. *Blood* 2011, 118:5218–5226
50. Nijmeijer B, van Schie M, Halkes C, Griffioen M, Willemze R, Falkenburg J: A mechanistic rationale for combining alemtuzumab and rituximab in the treatment of ALL. *Blood* 2010, 116:5930–5940